Microstructural development of high temperature deformed AZ31 magnesium alloys

Peiman Shahbeigi Roodposhti *, Apu Sarkar, Korukonda Linga Murty

North Carolina State University, USA

A B S T R A C T

Due to their significant role in automobile industries, high temperature deformation of Mg–Al–Zn alloys (AZ31) at constant stress (i.e. creep) were studied at a wide range of stresses and temperatures to characterize underlying deformation mechanism, dynamic recrystallization (DRX) and dislocation density evolution. Various microstructures (e.g. grain growth & DRX) are noted during steady-state creep mechanisms such as grain boundary sliding (GBS), dislocation glide creep (DGC) and dislocation climb creep (DCC). Although a combination of DRX and grain growth is characteristic of low stacking fault energy materials like Mg alloys at elevated temperatures, observation reveals grain growth at low strain-rates (GBS region) along with dynamic recovery (DRV) mechanism. X-Ray Diffraction (XRD) analysis revealed a decrease in dislocation density during GBS region while it increased under dislocation based creep mechanisms which could be related to the possible DRV and DRX respectively. Scanning Electron Microscopic (SEM) characterization of the fracture surface reveals more inter-granular fracture for large grains (i.e. GBS region with DRV process) and more dimple shape fracture for small grains (i.e. DGC & DCC region with DRX).

1. Introduction

Mg–Al alloys and in particular Mg–3Al–1Zn have aroused significant interest in last two decades [1–9] due to their wide uses in automotive industries. Like other hcp crystal structure materials, they are categorized as difficult to work alloys at room temperatures [10]. Researchers tried to analyze high temperature deformation behavior of these alloys to improve their mechanical properties at elevated temperatures. It is well known that their poor creep resistance at higher temperatures is due to intermetallic phase dissolving in the matrix [11,12] which leads to clamping load reduction in bolted joints in power-train components of automobiles [6]. Previous investigations revealed various mechanisms to be indicative during high temperature deformation of magnesium alloys [11] with the strain-rate related to the applied stress by well-known power-law equation:

$$\dot{\varepsilon} = A\sigma^n \exp\left(\frac{-Q}{RT}\right), \qquad (1)$$

where n is the stress exponent, A is a material constant, Q is the activation energy for creep, R is the gas constant and T is the absolute temperature. The stress exponent depends on the underlying creep mechanism: $n \sim 2$ is related to the grain boundary sliding, $n = 3–3.5$ dislocation glide and $n = 4.5–7.5$ is related to dislocation climb [6,11–19]. DRX is one of the most significant mechanisms for grain refinement and improved mechanical properties during hot working [20], which reduces the flow stress of deformation [21]. Unlike high stacking fault energy metals, DRX is a common phenomenon during high temperature deformation of low or medium stacking fault energy metals, such as magnesium [22–27]. In Mg–Al alloys, limited number of slip systems and higher grain boundary diffusion rate can also stimulate DRX [21]. Various investigations showed that during DRX new equiaxed grains appear on the preexistent grain boundaries when the dislocation density reaches a critical value [27–29]. Although there are some reports on the influence of primary grain size on DRX [21,30], new grain size is generally independent of the initial grain size and mostly related to the deformation conditions [21]. Like any recrystallization process (i.e. proceeding with nucleation and growth) recrystallization of fine grains is faster than in coarse grains due to higher nucleation sites for DRX [31]. It is well understood that by increasing the temperature and strain-rate more nucleation sites appear which leads to easier DRX and more grain refinement [32] while, stress, another essential parameter for DRX, does not influence the nucleation behavior and may strongly affect the kinetics of plane strain deformation [33].

* Corresponding author. Tel.: +1 919 757 7030; fax: +1 919 515 5115.
  E-mail address: pshahbe@ncsu.edu (P. Shahbeigi Roodposhti).

At higher temperatures the microstructure is more homogeneous albeit there is more grain growth due to higher grain boundary migration and diffusion [34].

Continuous DRX (CDRX) has been identified in Mg alloys [7,31,35–41] and in many cases a power law relationship has been shown to relate deformation conditions to the dynamically recrystallized grain size [30,42–45]. During CDRX unlike conventional DRX, production of high angle grain boundaries during high temperature deformation has no influence on the nucleation and growth of grains on preexisting grain boundaries [21].

In this study, the creep deformation of AZ31 magnesium alloy was investigated at high temperatures ranging from 503 to 623 K (i.e. 0.53–0.68T_m) to evaluate underlying deformation mechanisms, grain size distribution and the existence of DRX at different stages. XRD technique has been employed to measure dislocation density at various stages and relate it to possible DRV and DRX.

2. Experimental procedure

A commercial grade AZ31 magnesium alloy with chemical composition of Mg–2.8Al–1.1Zn (wt%) in the form of a rod with dimensions of 1″ × 1″ × 12″ has been used in this research. Dog-bone type tensile specimens of 25 mm gage length (Fig. 1) were machined out of the rod. The samples were annealed for 2 h in argon atmosphere at 450 °C and furnace cooled to room temperature to attain homogeneous equiaxed grains. Three dimensional microhardness tests were made to ascertain that it is fully homogenized in all directions. High temperature creep tests at constant load were performed at 230 °C, 270 °C and 350 °C with the tensile axis parallel to the rolling direction. The experimental setup used to perform direct load creep tests consists of an extensometer and a Linear Variable Differential Transducer (LVDT) to measure the axial strain. A three zone split furnace was used to heat the sample. The specimens were held for 30 minutes to equilibrate at the testing temperature prior to loading. Creep tests were performed under stresses ranging from 1 MPa to 70 MPa for dwell times of 3 min up to few weeks. The creep tests were performed in unprotected (air) atmosphere and no oxidation appeared on the surface of the sample after the test. By the end of the tests, the specimens were cooled under load to room temperature to preserve final stage crept microstructure. True strain (ε) and true stress (σ) are related to the total displacement of the extensometer (ΔL) and the initial dimensions of sample (A_0 and L_0) through the basic formulae of $\varepsilon = \ln(1 + \Delta L/L_0)$ and $\sigma = (F/A_0)(1 + \Delta L/L_0)$ respectively. The microstructure and chemical composition of the sample were examined by a Hitachi-3200 Scanning Electron Microscope (SEM) equipped with X-ray Energy Dispersive Spectroscopy (EDS). XRD experiments on the starting and deformed samples were carried out using the Panalytical Empyrean X-Ray Diffractometer equipped with advanced PlXcel 1D detector. In situ high temperature XRD study was performed on the starting Mg alloy sample to investigate the thermal stability of the precipitates. Sample was placed inside a furnace at a vacuum of 5×10^{-5} torr and heated from ambient temperature to 450 °C at a rate of 5 °C/min. Diffraction profiles were recorded at 50 °C interval. For optical microscopy, the specimens were polished with SiC abrasive paper followed by intermediate polishing using 9 μm, 3 μm and 1 μm glycol-based polycrystalline diamond suspensions with 3 separate non-woven textile polishing cloths. To clean the sample after each step of polishing, the surface was rinsed with ethanol and then sonicated into an ethanol bath to wash away any residual contaminates from the surface. For final polishing, 0.04 μm colloidal silica was used along with napless polyurethane cloth. Samples were finally etched for 5s with a solution of 5 ml Picric acid, 10 ml acetic acid, 10 ml H_2O and 70 ml ethanol. To prepare Transmission Electron Microscopy (TEM) foils, samples were thinned by standard twin jet electropolishing technique with a solution of 5% $HClO_4$ and 95% ethanol.

3. Results and discussion

Optical micrograph of an annealed sample, grain size distribution and micro-hardness values along the three directions are shown in Fig. 2. It is clear that the material has an equiaxed grain structure with average linear intercept grain size (ALIGS) of ~17 μm and homogeneous mechanical properties in all 3 dimensions.

Fig. 3 shows the TEM microstructure of the annealed sample and corresponding diffraction pattern for matrix and precipitates. Diffraction pattern of the matrix with zone axis of $[10\bar{1}0]$ is indicative of the hcp crystal structure, while the precipitates have different crystal structures.

A large number of creep tests have been performed at stresses ranging from 1 to 70 MPa. Depending on the creep conditions (stress and temperature) a wide range of creep curves with very low to large primary creep (stage I) regimes was noted. During this stage creep rate continuously decreased as a function of time followed by steady-state creep regime (stage II) in which the strain-rate remained constant. With increasing stress and/or temperature the secondary stage becomes shorter while the sample experiences a large primary creep [6]. Fig. 4 includes creep curves at low and high stresses along with the corresponding strain-rate vs. time plots.

Fig. 5a shows a double log plot of steady-state strain-rate vs. normalized stress (σ/E, E being temperature dependent elastic modulus) of several creep tests conducted at different temperatures and stresses. The temperature dependence of elastic modulus was obtained from Eq. (2) [13].

$$E = 2.6 \times (1.92 \times 10^4 - 8.6T) \text{ MPa } (T \text{ in K}) \tag{2}$$

It is evident from the plot (Fig. 5a) that the data for steady-state or minimum strain-rate vs. normalized stress follows power law behavior for a particular temperature. However, the slope changes with stress indicating transitions in creep mechanism(s). Data points in Fig. 5 are fitted using Eq. (1) to determine the stress exponent (n). Three different values of n were obtained: $n \sim 2$ related to the grain boundary sliding at low stresses, $n \sim 3$ dislocation glide at intermediate stresses and $n \sim 7$ dislocation climb in high stress regime. Similar results were obtained for other Mg alloys [6,13]. A semi-log plot of steady-state strain-rate vs. inverse of temperature (T^{-1}, T in K) is used to determine the activation energy for creep at different regions. Fig. 5b shows the data for regions I, II and III corresponding to low, intermediate and high stresses. An activation energy value of 87 kJ/mol was obtained for region I, 119 kJ/mol for region II and 122 kJ/mol for region III. Activation energy value of 87 kJ/mol is identified with that for grain boundary diffusion (Q_{GB}) in Mg and its alloys while the higher value of 120 kJ/mol in regions II and III is close to that for self-diffusion [13]. The well-known Zener–Hollomon parameter (Z) can relate the strain-rate and temperature ($Z = \dot{\varepsilon}(\exp Q/RT)$). Fig. 5c and d reveals the Zener–Hollomon parameter vs. dimension-less stress with $Q = Q_{GB}$ and $Q = Q_L$ respectively.
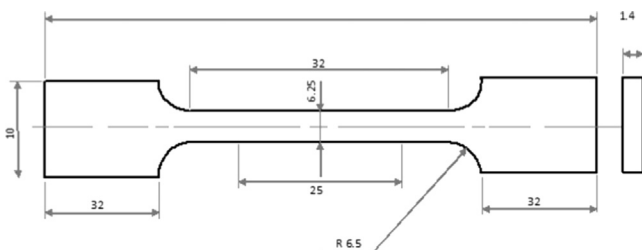

Fig. 1. Schematic of the dog-bone shaped tensile specimens.